Final Report 1992:
Advanced Water Window X-Ray Microscope Design and Analysis
Purchase Order No. H-08073D

D. L. Shealy, C. Wang, W. Jiang, J. Lin
Department of Physics
310 Campbell Hall
The University of Alabama at Birmingham
Birmingham, AL 35294-1170
Internet: shealy@uabphy.phy.uab.edu

September 11, 1992

Abstract

This project has been focused on the design and analysis of an advanced water window soft-x-ray microscope. These activities have been accomplished by completing three task contained in the Statement of Work of . .s contract. The new results from this work confirm that in order to achieve resolutions greater than three times the wavelength of the incident radiation, it will be necessary to use aspherical mirror surfaces and to use graded multilayer coatings on the secondary in order to accommodate the large variations of the angle of incidence over the secondary when operating the microscope at numerical apertures of 0.35 or greater. These results have been included in a manuscript entitled "Design and analysis of a fast, two-mirror soft-x-ray microscope," which is to appear in Proc. SPIE, vol. 1741-05, 1992, and which is enclosed in the Appendix of this report.

1 Introduction:

In support of the NASA/MSFC Advanced Water Window X-ray Microscope effort, this work addressed three task. Task 1 (Advanced Water Window Imaging X-Ray Design) focused on determination of system parameters of a microscope which could be fabricated with a goal of being able to record on film images with a resolution of two to three times the wavelength of the incident radiation $(2-3\lambda)$. Task 2 (Model and Evaluate Multilayer Coatings) proposed that efforts should be directed at identifying optimal material for maximization of reflectivity and throughput within the $23 - 44$ Å regime, which is known as the "water window." Task 3 (Properties of Biological Specimens) proposed that the physical and x-ray absorption characteristics of biological specimens be used to optimize the source, optics and detector design for maximization of contrast and resolution of the microscope when used with whole cells. Initial time estimates proposed that 50 per cent of the effort would be directed towards Task 1 and 25 per cent of the effort on Task 2 and Task 3. In order to achieve a much higher resolution of 1.4λ and to do some tolerance analysis for the Head-Schwarzschild microscope configurations, more effort was allocated to Task 1 and less to Task 3. The reader of this report is encouraged to read the manuscript presented in the Appendix first. The next section of this report contains some results not presented in this paper. Then, recommendations and conclusions of this entire project will be presented in the third section of this report.

2 Results

Figure 1 presents a geometrical configuration of the Head-Schwarzschild microscope. When configuring a reflecting microscope system, the magnification is normally determined by the object and detector resolutions. Equations 1 - 3 from the Appendix enable one to evaluate the Schwarzschild microscope parameters when the magnification, m, and radius of curvature of the secondary, R_2, are given. Table 1 presents a tabulation of Schwarzschild microscope parameters when $R_2 = 10cm$ and m ranges from 2 to $200x$. When alternate values of R_2 are used, all spatial dimensions scale linearly with R_2. Figure 2 presents an alternate version of the dependence of the numerical aperture of a $30x$ spherical Schwarzschild microscope versus the secondary

radius of curvature for different diameters of the primary mirror, as presented in the Appendix.

Using the equations presented in section 3 of the Appendix, data for the aspherical mirror surfaces of a Head-Schwarzschild microscope can be evaluated when the magnification and the spacings between the object and primary, image and secondary, and the two mirror surfaces are given. Using a linear least squares fitting technique, the mirror surface data can be fitted by surface equations of the form

$$z(h) = \frac{ch^2}{1 + \sqrt{(1 - c^2 h^2)}} + \sum_{i=4,6}^{i\,max} A_i h^i \tag{1}$$

where c is the vertex curvature, h is the height of a ray from the optical axis, A_i are the aspherical deformation coefficients, which range in number depending of the fitting approach. For the aspherical coefficients presented in Table 2, $i\,max = 18$, and eight aspherical deformation terms were considered in this fit. Figure 3 presents the sine wave MTF for the microscope described by the data in Table 2: System 1.

Using a nonlinear least squares fitting program, efforts have been directed at simplifying the fitted Head surface equations. Table 2: System 2 presents surface fitting data for a 30x Head-Schwarzschild system designed to operate with $NA = 0.35$, zero conic constant and a minimum number of aspherical deformation coefficients such that diffraction limited performance is achieved. Figure 4 presents the MTF for the microscope described by Table 2: System 2. Note that the microscope described by Table 2: System 2 yields diffraction limited performance. However, if one compares the performance shown in Fig. 3 to Fig. 4, one should note that Table 2: System 1 and Fig. 3 are for a Head-Schwarzschild microscope with $NA = 0.4$; whereas, Table 2: System 2 and Fig. 4 are for a slower system. Table 2: System 3 presents surface data for a 30x Head-Schwarzschild system ($NA = 0.35$) with a non-zero conic constant. Note that the conic constant enables the nonlinear least squares fitting program to obtain a good fit of the Head surfaces when only two aspherical deformation coefficients are considered. Figure 5 presents the MTF performance of the microscope described by Table 2: System 3. Note that all three representations of the 30x Head-Schwarzschild microscope considered have a secondary vertex radius of curvature of 5 cm.

For fast, two-mirror Head-Schwarzschild microscopes, the angle of inci-

3

dence varies more strongly over the secondary mirror than the primary. It appears necessary to use a graded 2d spacing for multilayers on the secondary for water window applications. For a $NA = 0.35$ Head-Schwarzschild microscope, the angle of incidence varies from $12° - 20°$. Figures 6 and 7 display the variation of the reflectivity of a multilayer as a function of the angle of incidence where the multilayer was optimized for three different design values of the angle of incidence $(0, 20° , 40°)$. For a modest number of multilayer pairs (25), the full-width half maximum of the reflectivity allows a $10°$ variation in the angle of incidence, which may enable use of a constant 2d spacing for the secondary multilayers; whereas, for a higher number of multilayer pairs (100), then the full-width half maximum of the reflectivity permits only a few degree variation in the angle of incidence. Note that for the cases considered in Figs. 6 and 7, a larger number of multilayer pairs gives a higher reflectivity. Before one can finalize a multilayer configuration for the Advanced Water Window Microscope, it will be necessary to know experimental constraints on making graded 2d multilayer mirrors.

Additional modeling and analysis of a $40x$ Head-Schwarzschild microscope system have been done where the vertex radius of curvature was considered to be equal to $5cm$. Table 3 presents the layout and linear least squared fitting data for this microscope operating at a $NA = 0.40$. Figure 8 shows the RMS blur radius versus the object height for a $40x$ Head-Schwarzschild microscope using different fitting formulas. It should be noted that all three fitting processes give very similar performance for the designed system. It is also indicated by these fitting processes that the surfaces of the Head-Schwarzschild microscope can be mathematically represented with high accuracy by some surface formulas.

After the designed surfaces have been fitted by some formulas, one can do the ray tracing and optical performance analyses for the Head-Schwarzschild systems. Normally, system alignment tolerances, such as, decentering, surface tilt and variance of the spacings, are done to investigate effects of the fabrication process on the system performance. In this study, attention has been focused on determining the feasibility of manufacturing Head aspherical surfaces, since the surface contour deviation become more important as the operating wavelength become shorter. In the following, an analysis of the performance of a $40x$ Head-Schwarzschild microscope will be presented, and the effects of manufacturing process of optical surfaces on the system performance will be investigated.

4

For the 40x Head-Schwarzschild microscope defined in Table 3, a resolution better than 50 Å is predicted to be the diffraction limited performance over an obje t field of 40μm when operating at a wavelength of 40 Å, as shown in Fig. 9. The sine wave MTF of this system and a spherical Schwarzschild microscope, operating at a wavelength of 100 Å, is shown in Fig. 10. Note from Fig. 10 that the Head-Schwarzschild microscope is near diffraction limited for $NA = 0.4$, which will provide significantly higher spatial resolution than a spherical Schwarzschild microscope for similar numerical aperture. The radial energy distribution for this 40x Head-Schwarzschild system is given in Fig. 11.

Although it has been demonstrated that the Head-Schwarzschild microscope can be designed to achieve diffraction limited performance over a large numerical aperture and the Head surfaces can be fitted very accurately, it can not be assumed that a Head-Schwarzschild microscope can actually be built to operate at these high numerical apertures, since the aspherical surfaces will require very accurate manufacturing of the surface contour. In addition to the system tolerances for alignment, analysis of the surface manufacturing tolerance become very important for soft-x-ray systems. In order to investigate the effects of the manufacturing process of optical surfaces on the performance of the designed system, some numerical simulations have been done. Based on an understanding of the manufacturing process, assume that the manufacturing process introduces some errors into the mathematically well fitted surfaces. Then, one can assume that a real surface can be described by the following formula:

$$z = f(x, y) + \delta(x, y) \tag{2}$$

where $f(x, y)$ represents the ideally fitted surface and $\delta(x, y)$ describes the manufacturing errors introduced into the surface contour.

For manufacturing a sysmmetric surface, the surface substrate usually is rotated about the symmetry axis while the cutting tool is milling on the surface, and the cutting tool should also be moved back and forth along the radial direction to cover the entire surface. Thus, it is reasonable to assume that the manufacturing surface errors are rotationally symmetric around the surface. In this simulation work, an approximately linear model for the manufacturing surface errors has been used and can be written as follows:

$$\delta(r) = kr[1 + c\sin(2\pi f_0 r)] \tag{3}$$

5

where $k = (Error_{max})/r_{max}$ is a constant that gives the maximum contour error on the surface, the constant c measures the contribution of rotational error effects, and f_0 gives the frequency of these rotational error effects. Figures 12-14 show the surface error functions with different values of parameters and the appropriate sine wave MTF for each case. It can be seen from Figs. 12-14 that the simulated surface errors contribute significantly to the system performance even though the maximum error value is only a quarter of wavelength.

3 Recommendations and Conclusions:

This investigator recommends that NASA fabricate a $30x$ Head-Schwarzschild microscope configured as listed in Table 2: System 3. All three systems described in Table 2 provide near diffraction limited performance. The substrate fabrication and test of System 3 appears to be more promising than the other two systems described in Table 2. In order to realize the resolution enhancement potential of these fast Head-Schwarzschild microscope, it will be necessary to use a divergent x-ray source with cone half-angle of at least $20°$, which suggest that a laser plasma system would be a good source configuration to enable the fast microscope to achieve the ultra high resolution of the diffraction limited performance of 1.4λ. The multilayer configuration of the Advanced Water Window Microscope can not be finalized until experimental constraints on making graded 2d multilayer mirrors are better understood.
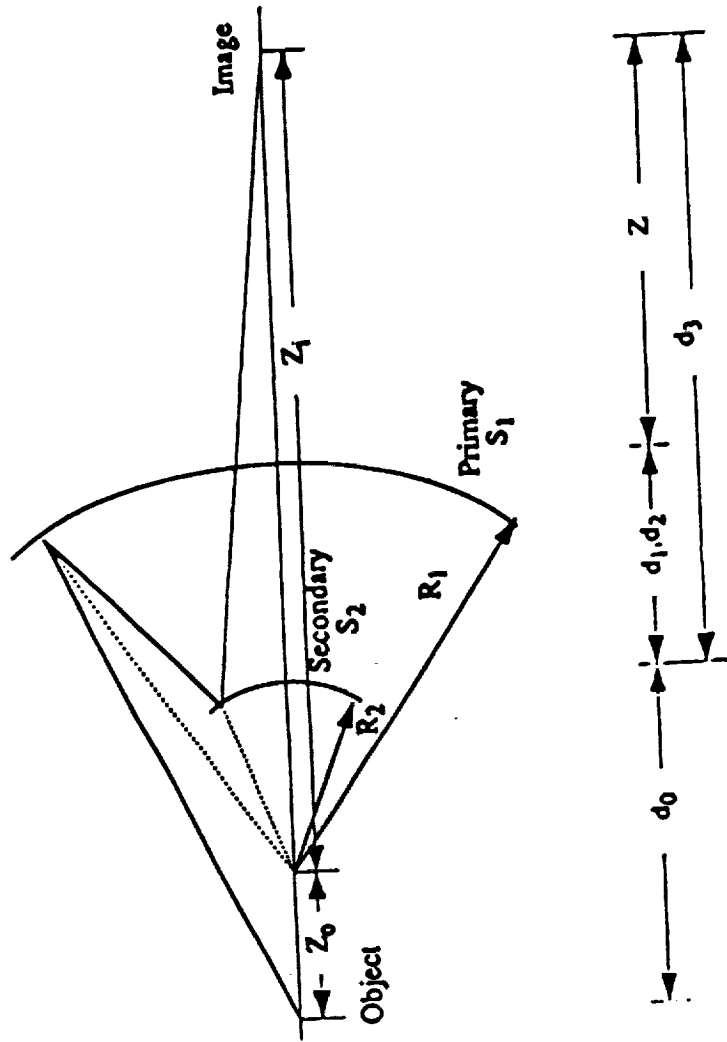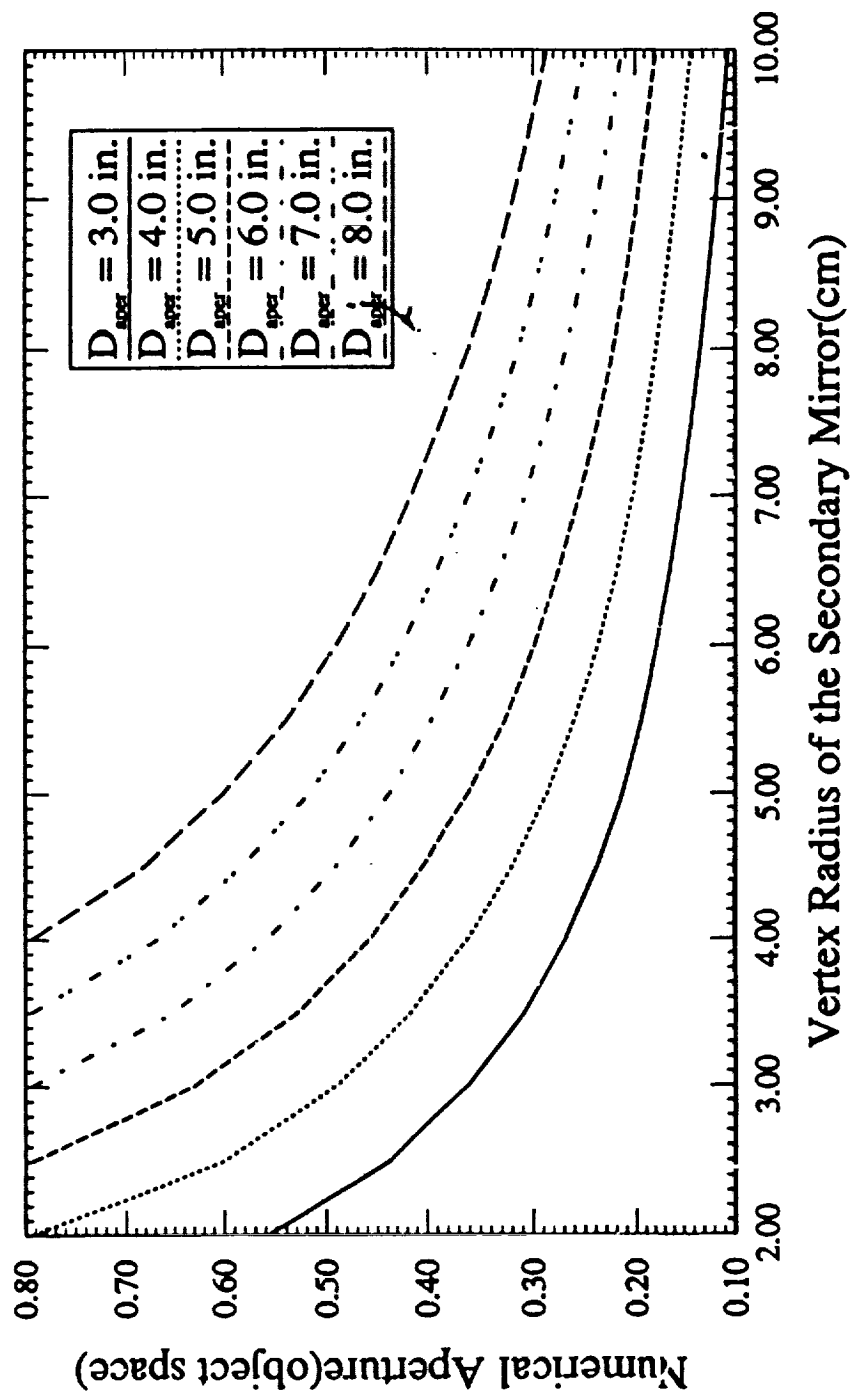
Image

Z_1

Primary
S_1

Secondary
S_2

R_1

R_2

Z_0

Object

d_0

d_1, d_2

Z

d_3

Fig. 1. Geometrical relations in a Head-Schwarzschild configuration.

30x Two-mirror Reflecting Microscope

$D_{apt} = 3.248$ in.
$M = 30x$

R_n	NA
2.00000	0.61054
2.50000	0.47606
3.00000	0.39205
3.50000	0.33383
4.00000	0.29090
4.50000	0.25787
5.00000	0.23164
5.50000	0.21028
6.00000	0.19256
6.50000	0.17760
7.00000	0.16481
7.50000	0.15374
8.00000	0.14407
8.50000	0.13555
9.00000	0.12798
9.50000	0.12122
10.00000	0.11513

Legend:
$D_{aper} = 3.0$ in.
$D_{aper} = 4.0$ in.
$D_{aper} = 5.0$ in.
$D_{aper} = 6.0$ in.
$D_{aper} = 7.0$ in.
$D_{aper} = 8.0$ in.

X-axis: Vertex Radius of the Secondary Mirror(cm)
Y-axis: Numerical Aperture(object space)

Fig. 2. Numerical aperture versus the secondary radius of curvature for different diameters of the primary mirror

DIFFRACTION MTF

OBJ.
DIAMETER (μ)

	0.0	0.035	0.050
T			
S			

NA = 0.4
$\lambda = 130$ Å

THROUGH FREQUENCY

THROUGH FOCUS

DIFFRACTION
LIMIT

1.0

0.2

2000.0

CYCLES/MM

1.0

0.2

-.100

0.0

0.100

MM

FIG. 3. MTF OF 30X HEAD MICROSCOPE (TABLE 1, SYSTEM 1).

DIFFRACTION MTF

REFERENCE 1190.0 CYCLES/MM

λ = 130 Å, NA = .35

OBJ.
DIAMETER (μ)

	0	35	50
T			
S			

THROUGH FOCUS

THROUGH FREQUENCY

DIFFRACTION
LIMIT

FITTING

CYCLES/MM

MM

FIG. 4. MTF OF 30X HEAD MICROSCOPE (TABLE 1, SYSTEM 2).

DIFFRACTION MTF

OBJ.
DIAMETER (µ)

REFERENCE1190.0 CYCLES/MM

$\lambda = 130\ \text{Å},\ NA = .35$

T ———— 0   35   50
S – – – –

THROUGH FREQUENCY

THROUGH FOCUS

1.0

0.2

1700.0

CYCLES/MM

DIFFRACTION
LIMIT

FITTING

1.0

0.2

-.050   0.0   0.050

MM
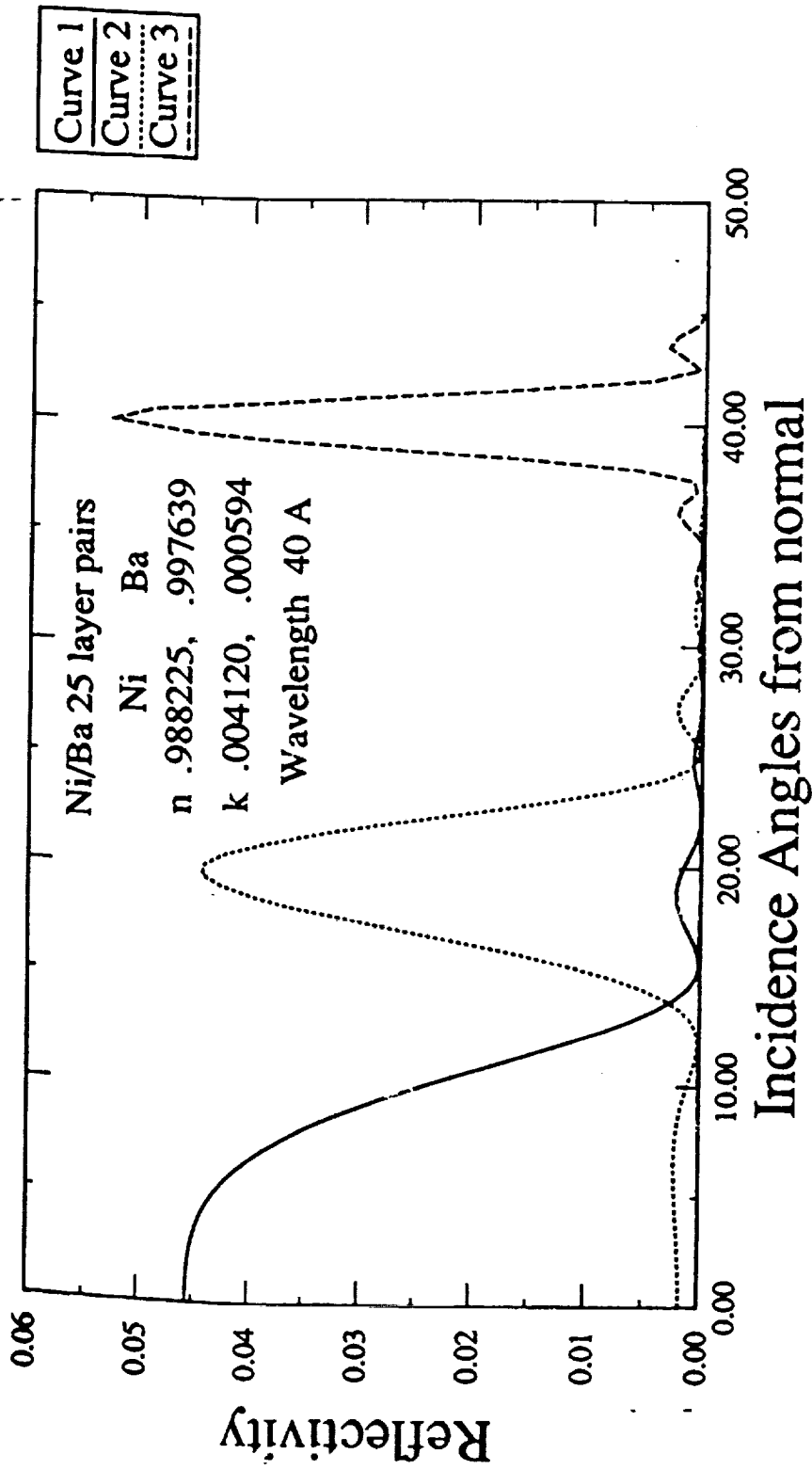
FIG. 5. MTF OF 30X HEAD MICROSCOPE (TABLE 1, SYSTEM 3).

Fig. 6. Multilayer reflectivity versus angle of incidence where the multilayer was optimized for three different design values of the angle of incidence (0, 20°, 40°).
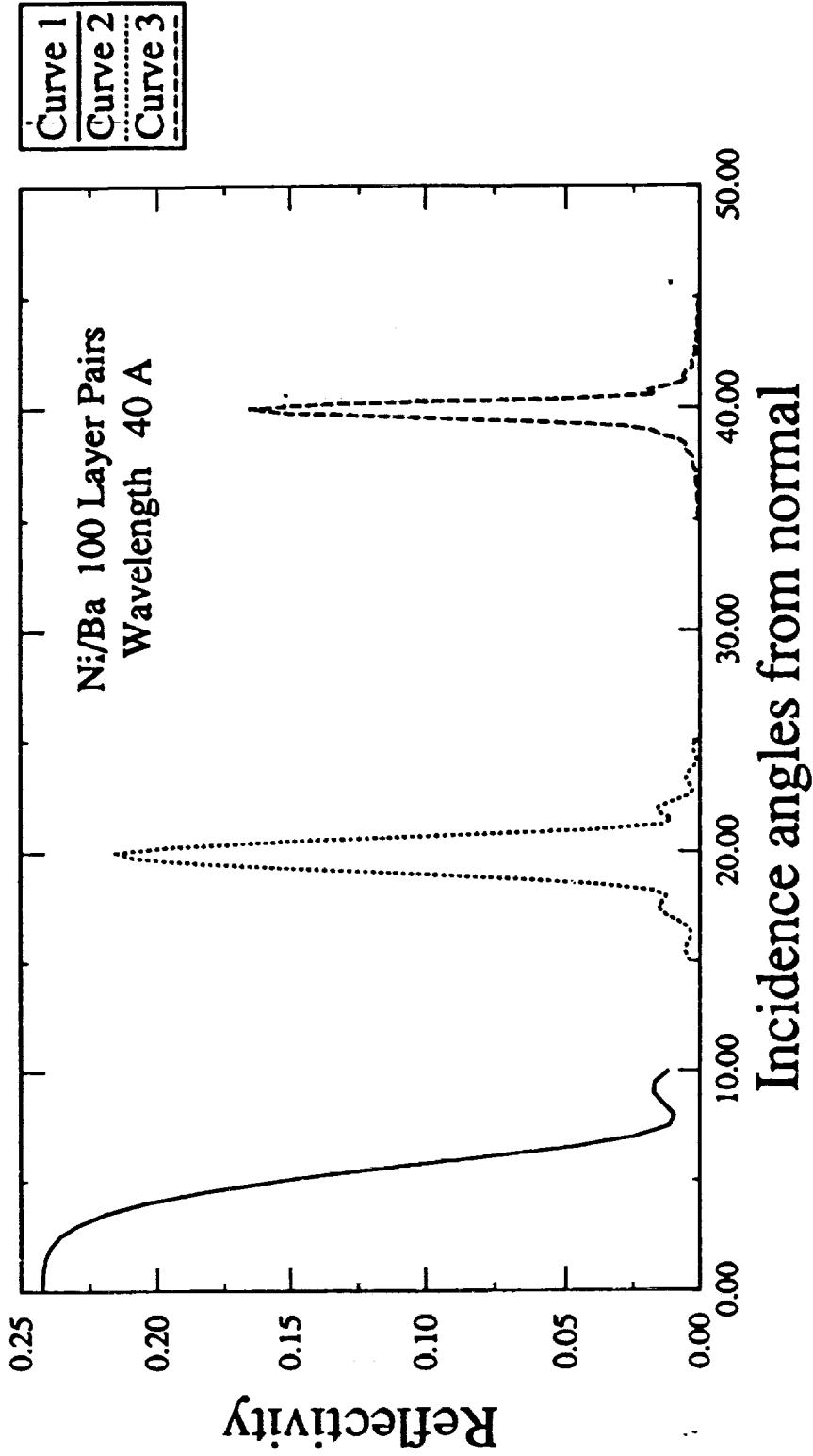
Fig. 7. Multilayer reflectivity versus angle of incidence where the multilayer was optimized for three different design values of the angle of incidence (0°, 20°, 40°).
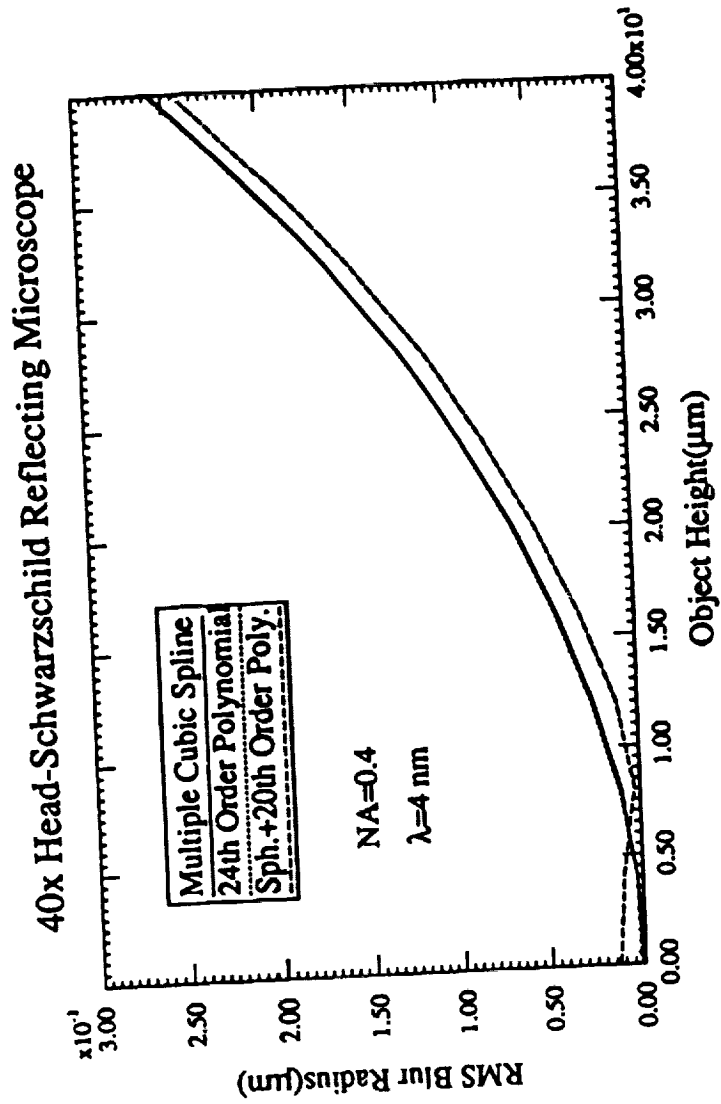
40x Head-Schwarzschild Reflecting Microscope

Multiple Cubic Spline
24th Order Polynomial
Sph.+20th Order Poly.

NA=0.4
λ=4 nm

RMS Blur Radius(μm)

Object Height(μm)

Fig. 8. RMS Blur radius versus object height for 40X Head-
Schwarzschild microscope.
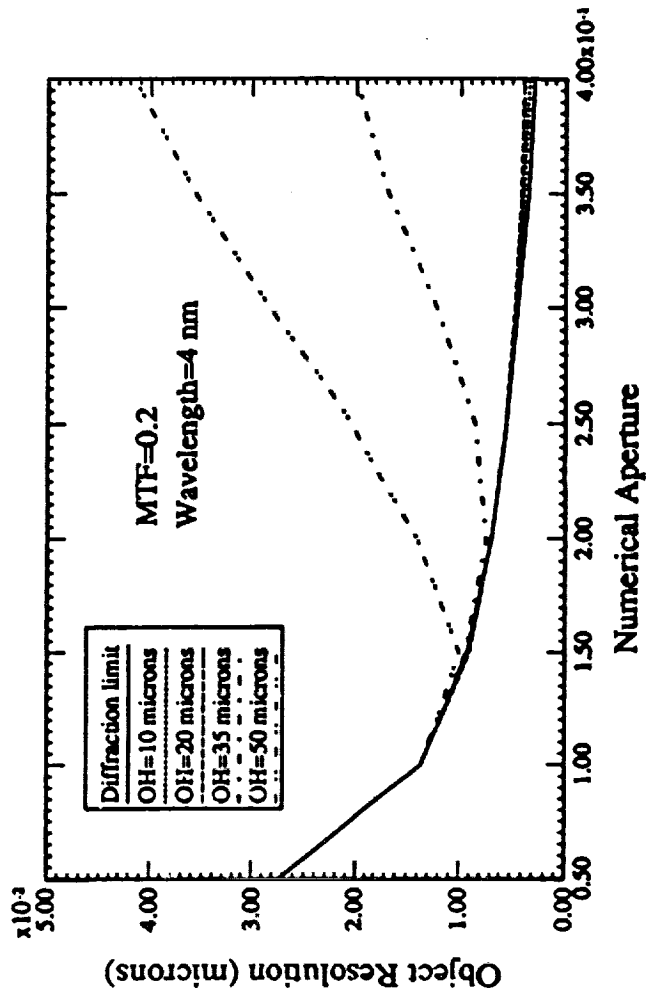
Fig. 9. Object resolution versus numerical aperture for 40X Head–Schwarzschild microscope.

NA=0.4
λ=10nm

Diffraction-limited
Obj.Height=0.0μm
Obj.Height=14.μm
Obj.Height=20.μm
Sph.Schwarzschild

Sine Wave MTF

1.00 0.90 0.80 0.70 0.60 0.50 0.40 0.30 0.20 0.10 0.00

0.00 0.20 0.40 0.60 0.80 1.00 1.20 1.40 1.60 1.80 2.00x10³
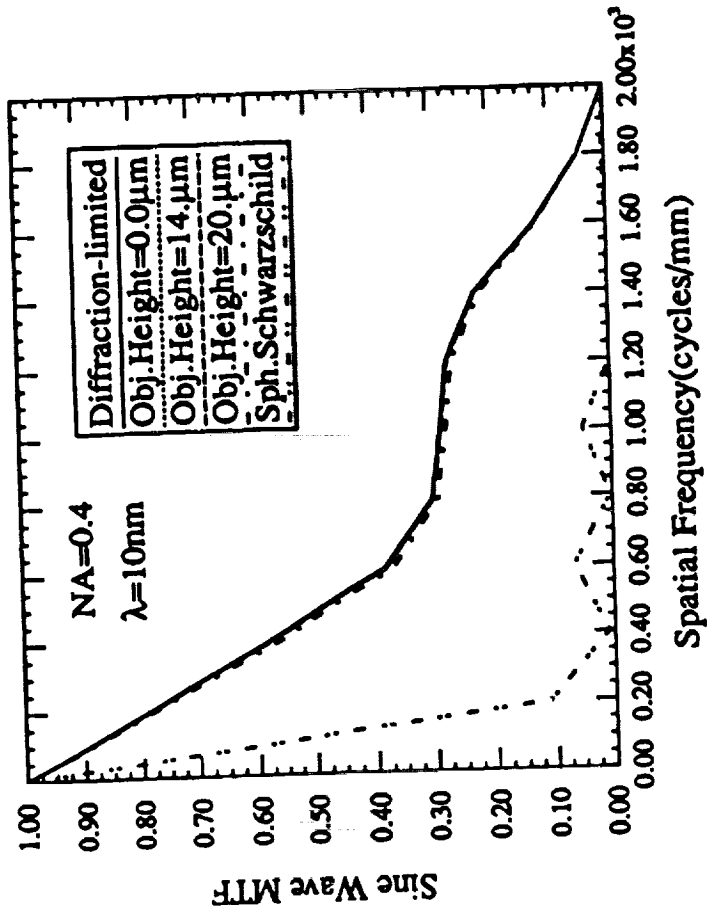
Spatial Frequency(cycles/mm)

Fig. 10. Sine wave MTF of 40X Head-Schwarzschild
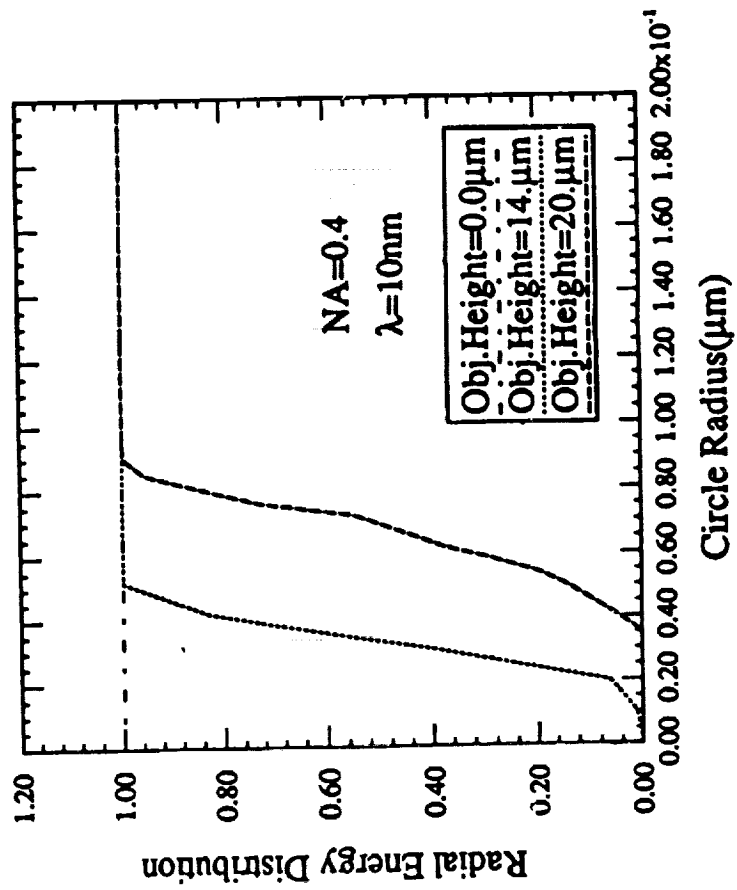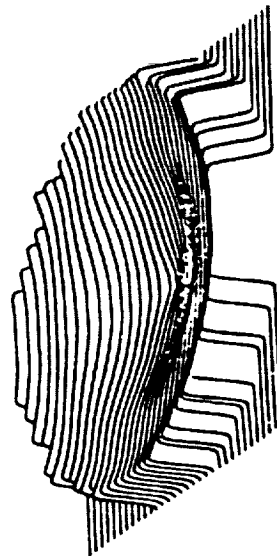and spherical Schwarzschild systems.

Fig. 11. Radial energy distribution for 40X Head-Schwarzschild microscope.

Error function $\delta(r)$ with C=0.01.
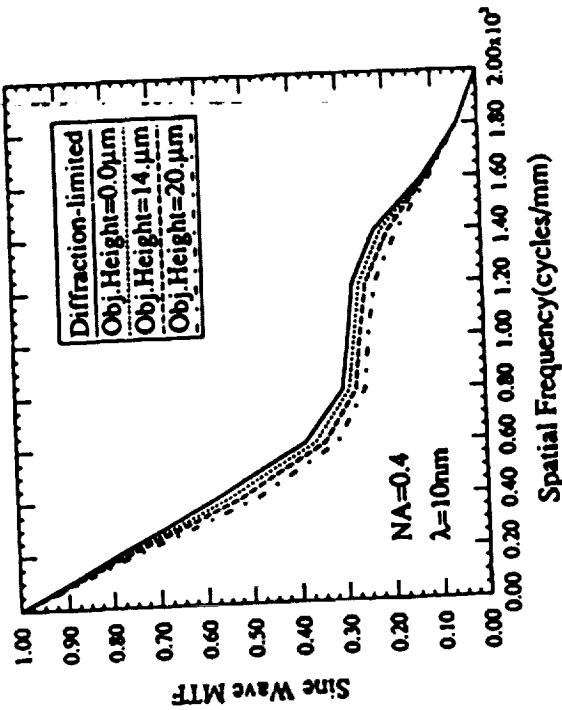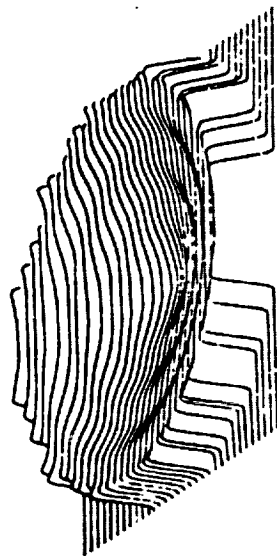
$$f_0 = 2/r_{max}$$

Fig. 13. Surface error function and Sine wave MTF for 40X Head-Schwarzschild microscope.

Sine Wave MTF

1.00
0.90
0.80
0.70
0.60
0.50
0.40
0.30
0.20
0.10
0.00

Diffraction-limited
Obj.Height=0.0μm
Obj.Height=14 μm
Obj.Height=20 μm

NA=0.4
λ=10nm

0.00 0.20 0.40 0.60 0.80 1.00 1.20 1.40 1.60 1.80 2.00x10³

Spatial Frequency(cycles/mm)

Error function $\delta(r)$ with C=0.01.
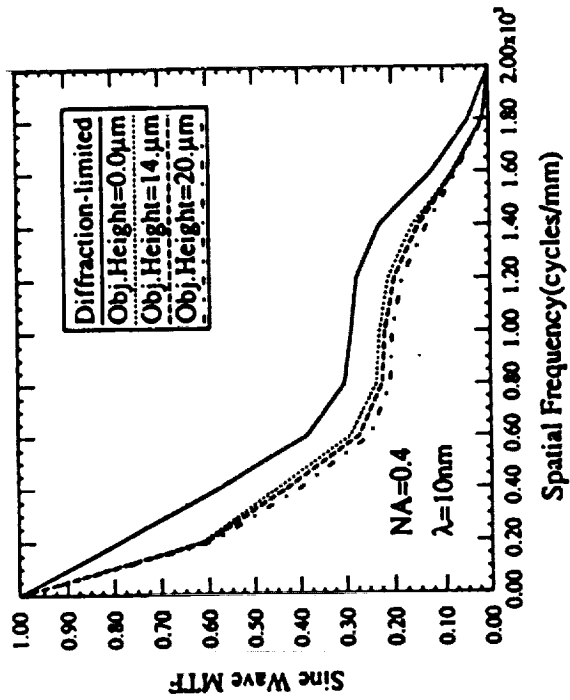
$f_o = 4/r_{max}$

Fig. 14.   Surface error function and Sine wave MTF for 40X Head-Schwarzschild microscope.

TABLE 1

Schwarzschild Microscope Parameters with $r_2 = 10$cm.

M(x)	r_1(cm)	Z_0(cm)	Z(cm)	L(cm)	f(cm)
2	109.0833	8.256939	−92.5694	117.3402	5.5046
3	58.2843	8.047379	−34.1421	66.3316	6.0355
4	45.5840	8.006406	−13.5584	53.5904	6.4051
5	40.0000	8.000000	0.0000	48.0000	6.6667
10	31.7929	8.023756	48.4446	88.2613	7.2943
15	29.6935	8.041505	90.9291	128.6641	7.5389
20	28.7361	8.052073	132.3053	169.0935	7.6686
30	27.8342	8.063728	214.0777	249.9756	7.8036
40	27.4027	8.069952	295.3954	330.8680	7.8731
50	27.1497	8.073812	376.5409	411.7644	7.9155
60	26.9835	8.076437	457.6027	492.6326	7.9440
70	26.8659	8.078337	538.6176	573.5619	7.9646
80	26.7784	8.079775	619.6036	654.4618	7.9800
90	26.7107	8.080902	700.5705	735.3621	7.9921
100	26.6567	8.081809	781.5242	816.2627	8.0018
120	26.5762	8.083177	943.4051	978.0645	8.0164
140	26.5190	8.084161	1105.2636	1139.8667	8.0268
160	26.4762	8.084902	1267.1081	1301.6692	8.0347
180	26.4430	8.085480	1428.9435	1463.4719	8.0408
200	26.4165	8.085944	1590.7724	1625.2748	8.0457

Table 2: TWO-MIRROR HEAD MICROSCOPE

General System Parameters:

Magnification = 30x

Wavelength = 130Å

NA(object) = 0.35

d_0 (object to secondary vertex distance) = 90.318625mm

d_1, d_2 (secondary to primary axial distance) = 89.1710mm

d_3 (secondary to image plane distance) = 1159.5595mm

System 1

Linear least squares techniques have been used to fit the numerical surface data of the Head microscope to formula representing a spherical term (conic constant = 0) plus 18th order polynomial representing the aspherical deformation terms.

	Primary	Secondary
Diameter (mm)	140.0	28.0
Hole Dia. (mm)	30.0	----
Vertex Radius (mm)	139.1710029	49.99999481
Conic Constant	0	0
A_4 (mm^{-3})	+4.169921D-12	-8.539853D-11
A_6 (mm^{-5})	-6.130163D-13	-3.643164D-9
A_8 (mm^{-7})	-3.886256D-17	-2.510754D-12
A_{10} (mm^{-9})	-4.762976D-21	-1.399772D-15
A_{12} (mm^{-11})	+4.134260D-25	-7.165030D-19
A_{14} (mm^{-13})	-8.866795D-29	-4.361604D-22
A_{16} (mm^{-15})	+6.371668D-33	-5.468617D-26
A_{18} (mm^{-17})	-2.737764D-37	-2.605799D-28

System 2

Nonlinear least squares techniques have been used to fit the numerical surface data of the Head microscope to a formula consisting of a spherical surface term (conic constant = 0) plus 10th order polynomial to represent the aspherical deformation terms.

	Primary	Secondary
Diameter (mm)	140.0	28.0
Hole Dia. (mm)	30.0	----
Vertex Radius (mm)	139.170963	50.0000012
Conic Constant	0	0
A_4 (mm^{-3})	+3.8477823D-12	+5.4950946D-10
A_6 (mm^{-5})	-8.9405110D-15	-4.4879182D-11
A_8 (mm^{-7})	+4.6907802D-19	+2.8078656D-14
A_{10} (mm^{-9})	-1.3328044D-22	-1.3305613D-16

System 3

Nonlinear least squares technique has been used to fit the numerical surface data of a Head microscope to a formula with a conic surface term plus 6th order polynomial representing the aspherical and non-conic deformation terms.

	Primary	Secondary
Diameter (mm)	140.0	28.0
Hole Dia. (mm)	30.0	----
Vertex Radius (rm)	139.170963	49.9999115
Conic Constant	+0.0029751487	-0.002862214
A_4 (mm^{-3})	+1.405927D-10	-1.826711D-9
A_6 (mm^{-5})	0	-4.739086D-11

Table 3. System parameters for a 40x Head-Schwarzschild x-ray microscope
(Surfaces are described by numerical surface data).

Magnification ─ ─ ─ ─ ─ ─ ─ ─ ─ ─ 40.00

Primary mirror

Vertex radius of curvature	13.70135 cm
Outside diameter	15.48154 cm
Hole Diameter	6.15065 cm

Secondary mirror

Vertex radius of curvature	5.00000 cm
Outside diameter	3.133174 cm
Object diatance from secondary(s)	9.03498 cm
Mirror spacing(d)	8.70135 cm
Image distance from primary(Z)	147.69770 cm
Overall length(s+d+Z)	165.43403 cm

Surface fitting parameters for a 40x Head-Schwarzschild x-ray microscope

Parameters	Primary	Secondary
R (cm)	13.70135	5.00000
κ	0.00000	0.00000
A4 (cm-3)	-0.131933875294077E-10	-0.156219804107234E-08
A6 (cm-5)	-0.653559251498143E-09	-0.344527894030282E-05
A8 (cm-7)	-0.502613453611377E-11	-0.237241032375997E-06
A10 (cm-9)	-0.229789120653666E-13	-0.131383965886426E-07
A12 (cm-11)	-0.389598050507999E-15	-0.689544120055730E-09
A14 (cm-13)	0.410717288192075E-17	-0.323554697185727E-10
A16 (cm-15)	-0.724848991939541E-19	-0.251252179356824E-11
A18 (cm-17)	0.505378996406414E-21	0.370745140031913E-13
A20 (cm-19)	-0.205886119729607E-23	-0.158756829827209E-13

APPENDIX

Design and analysis of a fast, two-mirror soft-x-ray microscope

D. L. Shealy, C. Wang, W. Jiang, L. Jin
Department of Physics
University of Alabama at Birmingham
Birmingham, AL 35294-1170

R. B. Hoover
Space Science Laboratory
NASA/Marshall Space Flight Center
Huntsville, AL 35812

ABSTRACT

During the past several years, a number of investigators have addressed the design, analysis, fabrication, and testing of spherical Schwarzschild microscopes for soft-x-ray applications using multilayer coatings. Some of these systems have demonstrated diffraction limited resolution for small numerical apertures. Rigorously aplanatic, two-aspherical mirror Head microscopes can provide near diffraction limited resolution for very large numerical apertures. This paper summarizes the relationships between the numerical aperture, mirror radii and diameters, magnifications, and total system length for Schwarzschild microscope configurations. Also, an analysis of the characteristics of the Head-Schwarzschild surfaces will be reported. The numerical surface data predicted by the Head equations have been fit by a variety of functions and analyzed by conventional optical design codes. Efforts have been made to determine whether current optical substrate and multilayer coating technologies will permit construction of a very fast Head microscope which can provide resolution approaching that of the wavelength of the incident radiation.

1. INTRODUCTION

Due to the vacuum environment of a sample, conventional electron microscopes can not be used to investigate biological samples under natural conditions. X-ray microscopes provide a different way of studying samples with a resolution of several hundred angstroms.[1, 2, 3] Although diffractive zone plates[4] can be used to focus x-rays in a microscope with a resolution of about three hundred angstroms, there are some problems, such as, low diffraction efficiency and the high cost of making the zone plates, which seem to constrain zone plate x-ray microscopes from achieving resolutions of less than 100Å. The development of multilayer coatings[5, 6] provides the possibility of using multilayer coated mirrors for soft-x-ray microscopy studies with very high resolutions.

An important field for using high resolution soft-x-ray microscopy is cell biology. Many biological samples contain carbon based molecules in an aqueous environment. The water window[7] refers to the soft-x-ray wavelength region of 23 − 44Å in which water is relatively transparent and carbon is highly absorptive. This provides a possibility of studying the structure of DNA and macromolecules within living cells. In order to study microscopic features of biological objects, a multilayer coated, reflecting microscope has been proposed for use within the water window,[8, 9] where one would like to resolve features smaller than 100Å.[10] For a reflecting microscope, this

means that a numerical aperture of about 0.4 or greater is required to enable the system to achieve resolutions less than 100Å.

The Schwarzschild two-mirror system[11, 12] has been used for many microscopy and projection lithography applications over a wide range of the electromagnetic spectrum. Recently, the spherical Schwarzschild optics coated with multilayers have been used in soft-x-ray microscopy applications[8, 9, 13, 14, 15] and for projection lithography[16, 17] where linewidths of 500Å have been written on photoresist by AT&T Bell Labs. While operating within the 100 − 200Å region, diffraction limited performance has been obtained for a small numerical aperture ($NA \leq 0.15$) and over a small field of view.

In an effort to provide capabilities for using alternate configurations of two-mirror microscopes while only using third-order designs, Hannan[18] has presented a general analysis of a two conical mirror relay system which corrects third-order spherical aberration, coma, and astigmatism. The concentric, spherical Schwarzschild system is a special case of Hannan's formulation. Hannan's approach enables one to construct a two-mirror microscope where the two conical mirrors are used to overcome the constraint of concentric, spherical mirrors required in the conventional Schwarzschild system. However, the Hannan system does not provide for any higher order correction of aberrations and would likely not function well with a large NA. In order to increase the resolution, one can decrease the operating wavelength and/or increase the NA. To increase the NA and to control aberrations such that diffraction limited performance can be achieved, the authors have proposed using the aspherical Head microscope design.[19, 20]

A. K. Head[21] has used the aplanatism conditions to set up differential equations for the surfaces in a two-mirror imaging system such that all orders of spherical aberration and coma are zero. This means that the Head microscope should provide near diffraction limited performance for very large NAs over a small field of view. Analytical solutions of these two differential equations have been obtained but can not readily be used by conventional optical design codes to determine the performance of a Head microscope.

In this paper, a parametric study for a spherical Schwarzschild microscope has evaluated the relationships between NA, mirror radii and diameters, magnifications, and the total system length. Also, an analysis of the characteristics of the aspherical surfaces of a Head-Schwarzschild microscope will be presented, including a discussion of fitting several different functions to the mirror surface data. Then, the optical performance of a fast Head microscope has been analyzed by conventional optical design codes. Analyses of the Head surface shapes and variation of the angles of incidence over the mirror surfaces have been conducted to determine whether current optical substrate and multilayer coating technologies will permit construction of a very fast Head microscope which may provide resolution approaching that of the wavelength of the incident radiation.

2. SPHERICAL SCHWARZSCHILD MICROSCOPE

A third-order aplanatic design for a reflecting microscope can be made from two concentric spherical mirrors as shown in Fig. 1, if the mirror radii satisfy the Schwarzschild condition:

$$\frac{R_2}{R_1} = \frac{3}{2} - \frac{R_2}{Z_0} \pm \sqrt{\frac{5}{4} - \frac{R_2}{Z_0}} \tag{1}$$
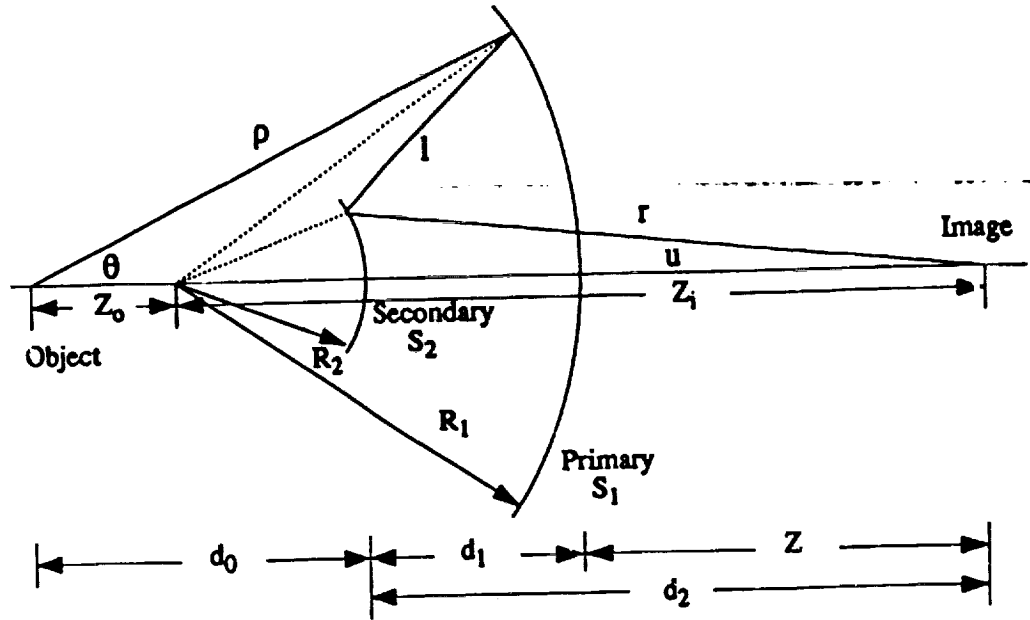
Figure 1: Geometrical configuration of a Head-Schwarzschild microscope.

where R_1 and R_2 are the radii of curvature of the primary and secondary mirrors, Z_0 is the distance from the object point to the center of curvature of the two mirrors, and the + sign in Eq. 1 is used when the magnification is greater than 5. Using paraxial optics relationships, the magnification of a spherical Schwarzschild microscope can be written as

$$m = \frac{-R_1 R_2}{(2R_1 Z_0 - R_1 R_2 - 2R_2 Z_0)}. \tag{2}$$

For a derivation and more discussion of the Schwarzschild condition, Eq. 2, and some ray tracing analyses, see Ref. [12]. It has also been shown[22] that a spherical Schwarzschild microscope does not have any third-order astigmatism while also satisfying the third-order aplanatism conditions.

When configuring a reflecting microscope system, the magnification is normally determined by object and detector resolutions. Therefore, Eqs. 1 and 2 are not in a convenient form for determining system parameters for a specific microscope. However, R_1 can be eliminated by combining Eqs. 1 and 2 to obtain:

$$\frac{R_2}{Z_0} = \frac{-m(m-1) + m\sqrt{(m-1)^2 + 4(m+1)^2}}{(m+1)^2} \tag{3}$$

where R_1 can now be evaluated as a function of m, using Eqs. 1 and 3. Using the mirror equation and Eqs. 1 - 3, one can evaluate the data in Table 1, which gives the Schwarzschild system parameters for a range of magnifications where $L(= Z_0 + Z_i)$ is the total length of a microscope and $Z(= Z_i - R_1)$ is the distance from the vertex of the primary mirror to the image plane. The data in Table 1 can be scaled linearly. For example, to obtain the system parameters for a

$M(x)$	$R_1(cm)$	$Z_0(cm)$	$Z(cm)$	$L(cm)$
10	31.7929	8.023756	48.4446	88.2613
20	28.7361	8.052073	132.3053	169.0935
30	27.8342	8.063728	214.0777	249.9756
40	27.4027	8.069952	295.3954	330.8680
50	27.1497	8.073812	376.5409	411.7644

Table 1: Schwarzschild Microscope Parameters for $R_2 = 10cm$.

microscope with a secondary radius of curvature of 5cm, then multiply the data in Table 1 by 0.5 to obtain the systems parameters for such a microscope.

While configuring a Schwarzschild microscope for a specific application, it is desirable to understand the relationship between the numerical aperture (NA) of the microscope, the magnification (m), the diameter of the primary mirror $(D_{1,apt})$, and the radius of curvature of the secondary mirror (R_2). For a spherical Schwarzschild microscope, it follows from the definition $NA = \sin\theta_{max}$ and Fig. 1:

$$NA = \frac{(D_{1,apt}/2)}{\sqrt{(D_{1,apt}/2)^2 + (Z_0 + R_1 - z_{1,max})^2}} \tag{4}$$

where from the equation of the primary mirror surface

$$z_{1,max} = \frac{(D_{1,apt}/2)^2}{R_1 + \sqrt{R_1^2 - (D_{1,apt}/2)^2}}. \tag{5}$$

Using Eq. 4 for the calculations, Fig. 2 displays the relationship between NA, m, and the ratio $(D_{1,apt}/R_2)$. One notes from Fig. 2 that NA is a much stronger function of $(D_{1,apt}/R_2)$ than of the magnification of the system. For a practical example of the usefulness of the data presented in Fig. 2, consider that based on the object and detector resolutions, one seeks to build a $30x$ microscope with a NA within the range of $0.3 - 0.4$. Then, from Fig. 2, it follows that $(D_{1,apt}/R_2)$ would need to be within the range of $2.05 - 2.70$. It is generally recognized[20] that a spherical Schwarzschild microscope can not perform with diffraction limited resolution for $NA \geq 0.15$, but the aspherical Head microscope, which will be discussed in the next section, will be able to operate with diffraction limited resolution for a very large NA.

Figure 3 presents a plot of the object space NA versus R_2 for different values of $D_{1,apt}$. The relationships between these parameters should be considered before building a specific configuration of a two-mirror microscope. After a determination of m and NA, then substrate fabrication, polishing, and multilayer coating technologies will drive a determination of R_2 and $D_{1,apt}$. Also, it should be noted that a determination of first-order system parameters is required before the aspherical mirror shapes can be evaluated for a Head-Schwarzschild microscope that can provide diffraction limited performance for very large NAs. For example, if one wishes to build a $30x$ microscope with a $12.5cm$ diameter primary, then Fig. 3 predicts that R_2 would decrease from
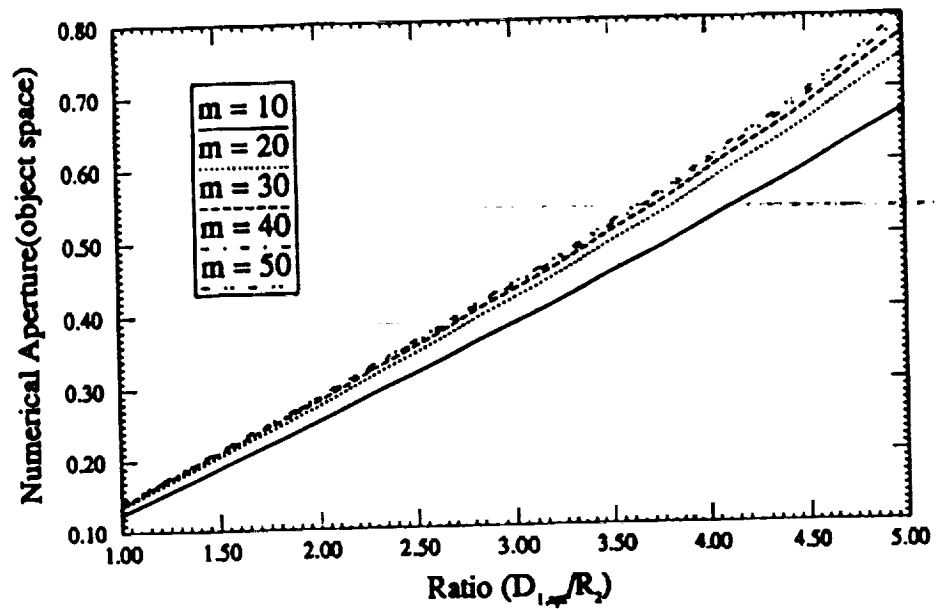
Figure 2: Numerical aperture of spherical Schwarzschild microscope versus the normalized primary mirror diameter($D_{1,apt}/R_2$) for different magnifications.
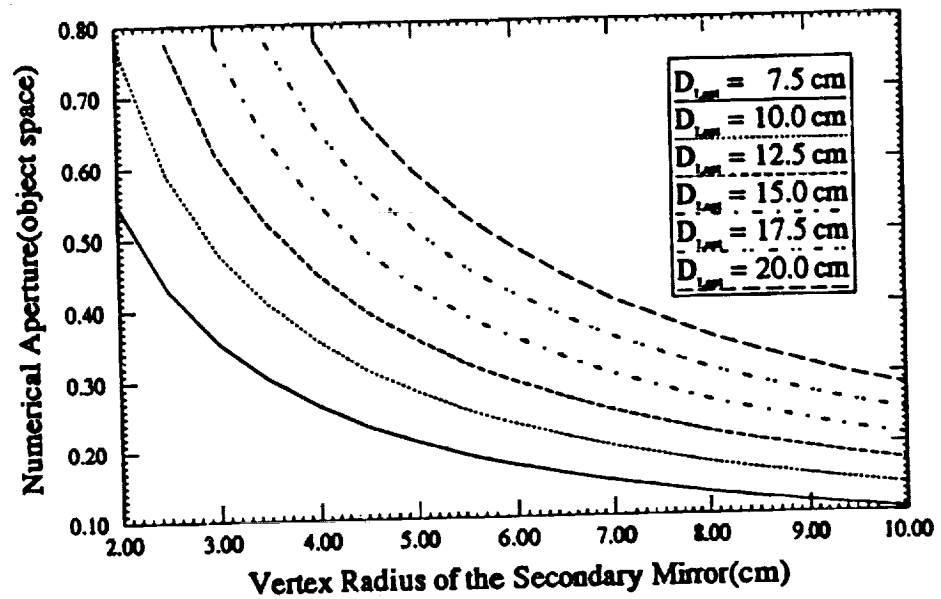

Figure 3: Numerical aperture of a 30x spherical Schwarzschild microscope versus the secondary radius of curvature(R_2) for different diameters of the primary mirror($D_{1,apt}$).

5.9cm to 4.5cm as NA is increased from 0.3 to 0.4. More specifically, Table 1 and Fig. 3 predict the following system first-order system parameters

$$m = 30x, \quad NA = 0.35, \quad L = 124.88cm, \quad R_1 = 13.917cm, \quad D_{1,apt} = 12.5cm, \quad R_2 = 5cm. \quad (6)$$

A microscope with these system parameters can be fabricated with current technology. However, one must examine the aspherical surfaces required of this system to provide diffraction-limited resolution with $NA = 0.35$ and a resolution of $Res = \lambda/(2NA) = 1.4\lambda$. Also, one must evaluate the variation of the angle of incidence over both mirrors to determine the nature of the multilayer coatings which will be required.

3. ASPHERICAL HEAD MICROSCOPE

In order to improve the optical performance of a third-order design, such as the spherical Schwarzschild microscope[12] or the conical microscope of Hannan[18], one often seeks an optical system which rigorously satisfies the Abbé Sine Condition for all rays:

$$\sin \theta = m \sin u \qquad (7)$$

and the constant optical path length condition:

$$\rho + r + l = \rho_0 + r_0 + l_0 \qquad (8)$$

where m is the microscope magnification, and the variables (ρ, r, l) are defined in Fig. 1. The constants (ρ_0, r_0, l_0) are the paraxial values of the corresponding variables. An optical system which satisfies Eqs. 7 and 8 is called an aplanat, which is free of all orders of spherical aberration and coma. In 1957, Head[21] presented an analytical solution in closed form for a two-mirror aplanat with finite object and image points, that is, a microscope or projection system. The primary and secondary mirror surfaces are specified by the following equations[19]:

Primary Microscope Mirror

$$\frac{l_0}{\rho} = \frac{(1+\kappa)}{2\kappa} + \frac{(1-\kappa)}{2\kappa} \cos\theta + \left(\frac{l_0}{\rho_0} - \frac{1}{\kappa}\right) \left(\frac{\gamma}{1+m}\right)^{-1}$$

$$* \left[\frac{\gamma-(1-m)}{2m}\right]^{\alpha} \left[\frac{\gamma-(m-1)}{2}\right]^{\beta} \left|\frac{(\kappa+1)\gamma}{2(m+1)} - \frac{(\kappa-1)}{2}\right|^{2-\alpha-\beta} \qquad (9)$$

where $\kappa = (\rho_0 + r_0)/l_0$, $\alpha = m\kappa/(m\kappa - 1)$, $\beta = m/(m - \kappa)$, and $\gamma = \cos\theta + \sqrt{m^2 - \sin^2\theta}$.

Secondary Microscope Mirror

$$\frac{l_0}{r} = \frac{(1+\kappa)}{2\kappa} + \frac{(1-\kappa)}{2\kappa} \cos u + \left(\frac{l_0}{r_0} - \frac{1}{\kappa}\right) \left(\frac{\delta}{1+M}\right)^{-1}$$

$$* \left[\frac{\delta-(1-M)}{2M}\right]^{\alpha'} \left[\frac{\delta-(M-1)}{2}\right]^{\beta'} \left|\frac{(\kappa+1)\delta}{2(M+1)} - \frac{(\kappa-1)}{2}\right|^{2-\alpha'-\beta'} \qquad (10)$$

where $M = 1/m$, $\alpha' = M\kappa/(M\kappa - 1)$, $\beta' = M/(M - \kappa)$, and $\delta = \cos u + \sqrt{M^2 - \sin^2 u} = M\gamma$.

It is straight forward to evaluate the mirror profiles of a Head microscope from Eqs. 9 and 10 for given input parameters $(m, r_0, l_0, and\ \rho_0)$, which follow from Fig. 1 and Table 1 using the following correspondence between Schwarzschild and Head parameters:

$$(L - Z) \Longrightarrow \rho_0, \quad (R_1 - R_2) \Longrightarrow l_0, \quad (L - Z_0 - R_2) \Longrightarrow r_0.$$

In order to use a conventional optical design program to analyze the performance of a Head microscope, it is necessary to fit an equation to the numerical surface data representing the primary and secondary mirror surfaces.

There are many ways to describe optical surfaces. Normally, optical surfaces are described by an equation with a conic term plus some aspherical deformation terms:

$$z = \frac{ch^2}{1 + \sqrt{1 - (1 + \kappa)c^2 h^2}} + \sum_{i=2}^{n} A_{2i} h^{2i} \tag{11}$$

where h is the radial distance of a point on the surface from the symmetry axis, $c(= 1/R)$ is the curvature of the vertex of the mirror, κ is the conic constant, and A_{2i} are the aspherical deformation coefficients. If κ and A_{2i} are zero, then Eq. 11 specifies that the surface is a sphere. If κ is not zero, but all A_{2i} are zero, then Eq. 11 represents a conical surface.

After evaluating the surface data for the primary and secondary mirrors in a Head microscope from Eqs. 9 - 10, then we have used both linear and nonlinear least squares fitting algorithms to determine the surface parameters of Eq. 11 such that the Head microscope can be very consistently modeled to satisfy the aplanatism conditions and to yield diffraction limited resolution for the desired NA. For a specific set of surface data, it is not clear initially how many aspherical deformation terms will be required or whether the conic constant is zero. Experience has shown that it is desirable to determine an approximate shape of the Head surfaces before doing extensive nonlinear least squares fitting. As a result of the initial values used in this work, the Head surfaces can be approximated by spherical Schwarzschild microscope surfaces with the corresponding surface parameters. Good representations for Head surfaces have been determined to have a small conic constant and one to two aspherical deformation ter ns or to have zero conic constant with four to eight aspherical deformation terms. It has been found that there are no unique representations for the fitting of a Head microscope surface, but all well behaved solutions have the same diffraction limited optical performance.

For example, using a nonlinear least squared fitting algorithm, a set of Head surface parameters is given in Table 2 for a $30x$ microscope with $NA = 0.35$ where the following axial spacings have been used

$$d_0 = 90.318625mm, \quad d_1 = 89.1710mm, \quad d_2 = 1159.5595mm. \tag{12}$$

The aspherical surfaces described in Table 2 represent surfaces which differ from a spherical surface by approximately one micron for a primary aperture radius of $70mm$, which corresponds to a $NA = 0.35$. Current substrate fabrication technologies should be able to make the mirror surfaces defined by Table 2. Figure 4 presents the MTF for the system given in Table 2 and Eq.12, which shows that this representation of the $30x$ Head microscope is diffraction limited.
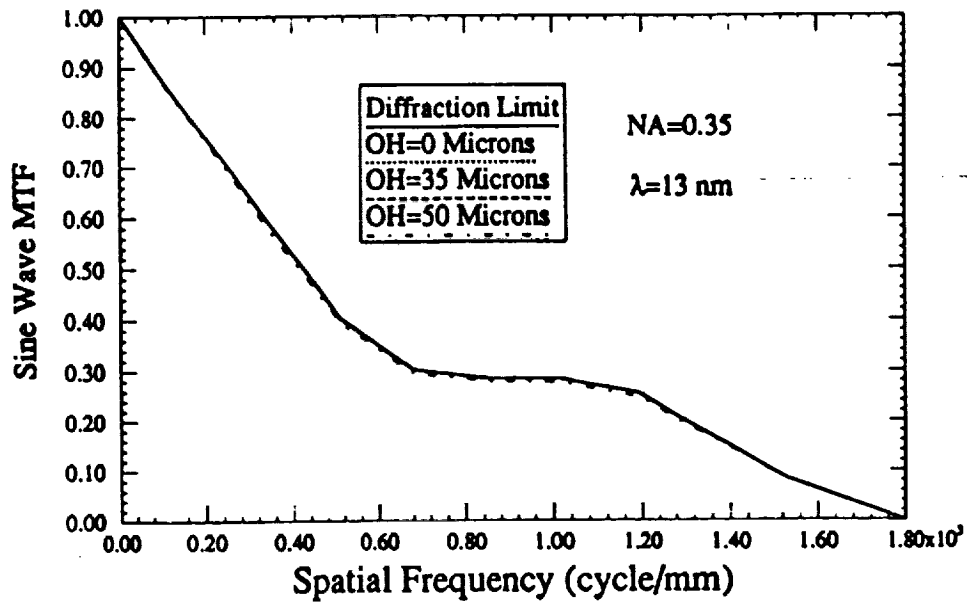
Figure 4: MTF vs the spatial frequency for $30x$ Head microscope where OH is the object height.

Variable	Primary	Secondary
Diameter(mm)	140.0	29.0
Hole Dia. (mm)	30.0	none
Vertex Radius (mm)	139.170963	49.999915
Conic Constant	0.0029751487	-0.002862214
A4 (mm-3)	1.405927D-10	-1.826711D-9
A6 (mm-5)	0	-4.739086D-11

Table 2: Nonlinear least squares technique has been used to fit the numerical surface data of a Head microscope to a formula with a conic surface term plus 6th order polynomial representing the aspherical and non-conic deformation terms.
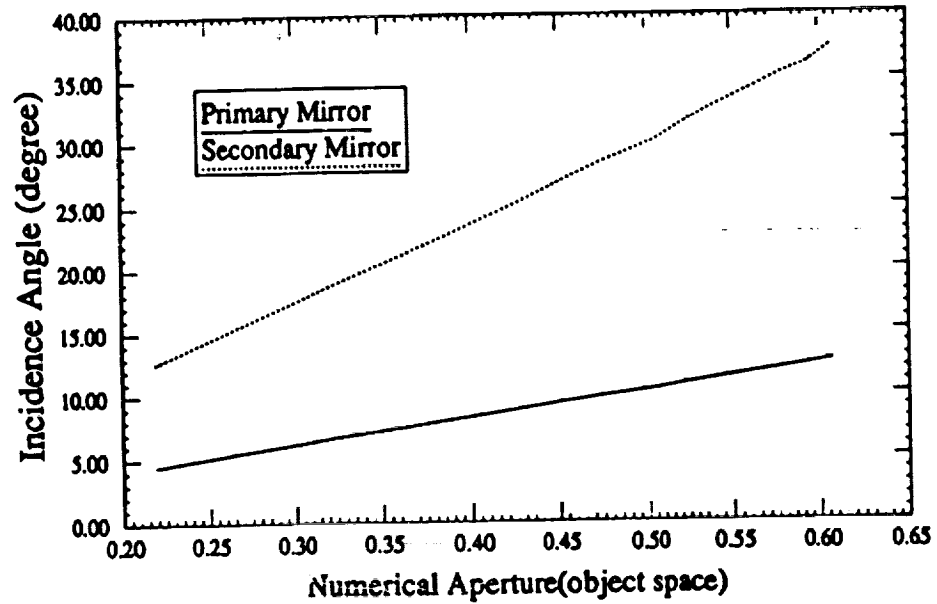
Figure 5: Variation of the angle of incidence over the Head surfaces of a $30x$ microscope versus the numerical aperture.

Next, it is important to determine whether it is possible to deposit multilayer coatings on these fast mirror surfaces. Figure 5 presents the variation of the angle of incidence on both the primary and secondary Head mirrors as a function of the microscope NA for the $30x$ Head microscope which is defined by Table 2 and Eq.12, where the diameter of the primary was increased to achieve larger NAs. It is evident from Fig. 5 that the angle of incidence varies more rapidly over the secondary than the primary. This strong variation of the angle of incidence over the secondary mirror has significant implications for the design and fabrication of multilayer coatings of a fast Head microscope.

Depending on how a multilayer is designed, peak reflectivities may only be maintained for a $5-10°$ variation in the angle of incidence over the multilayer. Therefore, conventional multilayer coatings can not be used for a very fast Head microscope. However, graded or segmented multilayer coatings may be used to coat the secondary mirror such that operation with acceptable reflectivity may be achieved for a wide range of NAs. To illustrate this concept, consider designing off-axis multilayers to work with a peak reflectivity for segments of the primary and secondary mirrors corresponding to the aperture of $NA = 0.45$ for a water window microscope using Ni/Ca multilayers.[23] Figure 6 illustrates this concept where the multilayer coatings on the primary have been optimized for a $8°$ angle of incidence with a d-spacing period of $20.3Å$ and ratio $(\frac{d_{Ni}}{d}) = 0.414$, and the multilayers on the secondary have been optimized for a $27°$ angle of incidence with a d-spacing period of $22.5Å$ and ratio $(\frac{d_{Ni}}{d}) = 0.32$. The multilayer optical constants for Ni[$n = 0.988225$, $k=0.004120$] and Ca[$n=0.999145$, $k=0.000278$] were evaluated from the Henke Tables.[24] It is interesting to note that for these segments of the mirror surfaces and for this configuration of multilayer coatings, this water window Head microscope would have a net reflectivity
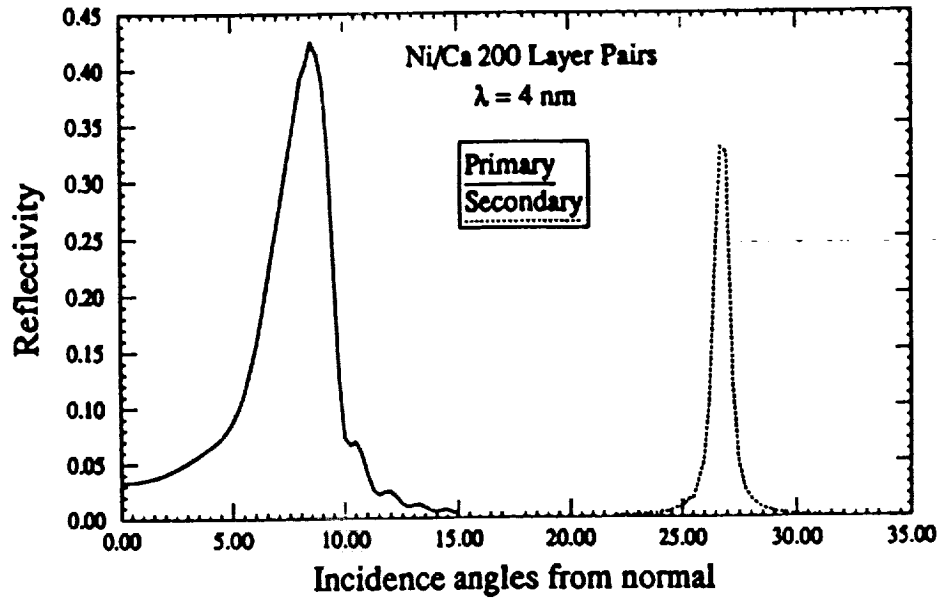
Figure 6: Reflectivity of proposed water window Head microscope versus the angle of incidence of radiation on mirror surfaces.

varying from a peak value of 14% to the full-width half-maximum value of 2.4%. By further optimizing the multilayers, one may be able to broaden the reflectivity versus angle of incidence peaks and to increase the system throughput. Efforts are also underway to identify different microscope configurations for which the angle of incidence does not vary as strongly over the secondary mirror surface as indicated in Fig. 5.

4. CONCLUSIONS

This work has summarized some useful relationships between NA, magnification, diameter of the primary mirror, radius of curvature of the secondary mirror, and the total length of the Schwarzschild configurations of a microscope. To achieve resolutions better than about 3λ, it is necessary to use aspherical Head surfaces to control higher-order aberrations. For a NA of 0.35, the aspherical Head microscope could provide diffraction limited resolution of 1.4λ where the aspherical surfaces would differ from the best fit sphere by approximately 1 micron. However, the angle of incidence would vary by about 6° over the secondary and 3° over the primary, which may require graded multilayer coatings to operate near peak reflectivities. For higher NAs, the variation of the angle of incidence over the secondary mirror surface becomes a serious problem which must be solved before multilayer coatings can seriously be considered for this application.

5. ACKNOWLEDGEMENTS

References

[1] *X-Ray Microscopy*, G. Schmal and D. Rudolph, Eds., Springer Series in Optical Sciences, vol. 43 (Springer-Verlag, New York, 1984).

[2] *X-Ray Microscopy II*, D. Sayre, M. Howell, J. Kirz, and H. Rarback, Eds., Springer Series in Optical Sciences, vol. 56 (Springer-Verlag, New York, 1987).

[3] *X-Ray Microscopy III*, A.G. Michette, G. R. Morrison, and C. J. Buckley, Eds., Springer Series in Optical Sciences, vol. 67 (Springer-Verlag, New York, 1990).

[4] M. R. Howells, J. Kirz, and D. Sayre, "X-ray microscopes," Sci. Am., 88-94, February, 1991.

[5] T. W. Barbee, Jr., "Multilayers for x-ray optical applications," in *X-Ray Microscopy*, G. Schmal and D. Ruldolph, Eds.,Springer Series in Optical Sciences, vol. 43 (Springer-Verlag, New York, 1984), 144-162.

[6] E. Spiller, "Enhancement of the reflectivity of multilayer x-ray mirrors by ion-polishing," Proc. SPIE 1160, 271-279 (1989).

[7] R. A. London, M. D. Rosen, and J. E. Trebes, "Wavelength choices for soft-x-ray laser holography for biological sample," Appl. Opt. 28, 3397-3404(1989).

[8] J. A. Trail, *A Compact Scanning Soft X-Ray Microscope*, Ph. D. Dissertation, Stanford University (1989).

[9] R. B. Hoover, D. L. Shealy, B. R. Brinkley, P. C. Baker, T. W. Barbee, Jr., and A. B. C. Walker, Jr., "X-ray imaging microscope for cancer research," in *Technology 2000*, NASA Conference Publication 3109, vol. 1, 73-82 (1991).

[10] R. B. Hoover, D. L. Shealy, B. R. Brinkley, P. C. Baker, T. W. Barbee, Jr., and A. B. C. Walker, Jr., "Development of the water window imaging x-ray microscope utilizing normal-incidence multilayer layer optics," Opt. Eng. 30.8, 1086-1093 (1991).

[11] K. Schwarzschild, "Untersuchungen zur geometrischen Optik, II; Theorie der Spiegelteleskope," Abh. der Königl. Ges. der Wiss. zu Göttingen, Math.-phys. Klasse, 9. Folge, Bd IV, No. 2 (1905).

[12] D.L. Shealy, D. R. Gabardi, R. B. Hoover, A. B. C. Walker, Jr., J. F. Lindblom, and T. W. Barbee, Jr., "Design of a normal incidence multilayer imaging x-ray microscope," J. X-Ray Sci. Technol. 1, 190-206 (1989).

[13] E. Spiller, "A scanning soft x-ray microscope using normal incident mirrors," in *X-Ray Microscopy*, G. Schmal and D. Rudolph, Eds., Springer Series in Optical Sciences, vol. 43 (Springer-Verlag, New York, 1984), 226-231.

[14] J. H. Underwood, R. C. C. Perera, J. B. Kortright, P. J. Batson, C. Capasso, S. H. Liang, W. Ng, A. K. Ray-Chaudhuri, R. K. Cole, G. Chen, Z. Y. Guo, J. Wallace, J. Welnak, G. Margaritondo, F. Cerrina, G. De Stasio, D. Mercanti, and M. T. Ciotti, "The MAXIMUM photoelectron microscope at the University of Wisconsin's Synchrotron Radiation Center," in *X-Ray Microscopy III*, A.G. Michette, G. R. Morrison, and C. J. Buckley, Eds., Springer Series in Optical Sciences, vol. 67 (Springer-Verlag, New York, 1990), 220-225.

[15] R. P. Haelbich, "A scanning ultrasoft x-ray microscope with multilayer coated reflection optics: first test with synchrotron radiation around 50eV photon energy," in *Scanned Image Microscope*, Ash, Ed. (1981), 413.

[16] D. W. Berreman, J. E. Bjorkholm, L. Eichner, R. R. Freeman, T. E. Jewell, W. M. Mansfield, A. A. MacDowell, M. L. O'Malley, E. L. Raab, W. T. Silfvast, L. H. Szeto, D. M. Tennant, W. K. Waskiewicz, D. L. White, D. L. Windt, and O. R. Wood II, "Reduction imaging at 14nm using multilayer-coated optics: printing of features smaller than $0.1\mu m$," J. Vac. Sci. Technol. B 8.6, 1509-1513 (1990).

[17] H. Kinoshita, K. Kurihara, Y. Ishii, and Y. Torii, "Soft-x-ray reduction lithography using multilayer mirrors," J. Vac. Sci. Technol. B 7.6, 1648-1651 (1989).

[18] P. G. Hannan, "General analysis of two-mirror relay systems," Appl. Opt. 31.4, 513-518 (1992).

[19] D. L. Shealy, W. Jiang, and R. B. Hoover, "Design and analysis of aspherical multilayer imaging x-ray microscope," Opt. Eng. 30.8, 1094-1099 (1991).

[20] D. L. Shealy, C. Wang, W. Jiang, and R. B. Hoover, "Design and analysis of soft-x-ray imaging microscopes," Proc. SPIE 1546, 117-124 (1991).

[21] A. K. Head, "The two-mirror aplanat," Proc. Phys. Soc. LXX, 10-B, 945-949 (1957).

[22] P. Erdös, "Mirror anastigmat with two concentric spherical surfaces," JOSA 49.9, 877 (1957).

[23] P. A. Kearney, J. M. Slaugher, and C. M. Falco, "Materials for multilayers x-ray optics at wavelengths below 100Å," Opt. Eng. 30.8, 1076-1080 (1991).

[24] B. L. Henke, P. Lee, T. J. Tanaka, R. L. Shimabukuro, and B. K. Fujikawa, *Atomic Data and Nuclear Data Tables*, vol. 27.1 (Academic Press, New York, 1982, Second Printing, 1987).

END

DATE

FILMED

OCT 23 1992